molecular pharmaceutics

articles

Synthesis, Characterization, and Gene Delivery of Poly-L-lysine Octa(3-aminopropyl)silsesquioxane Dendrimers: Nanoglobular Drug Carriers with Precisely Defined Molecular Architectures

Todd L. Kaneshiro, Xuli Wang, and Zheng-Rong Lu*

Department of Pharmaceutics and Pharmaceutical Chemistry, University of Utah, Salt Lake City, Utah 84108

Received April 6, 2007; Revised Manuscript Received June 22, 2007; Accepted June 22, 2007

Abstract: Macromolecules with defined nanosizes—nanoglobules—were synthesized and characterized as novel drug carriers with precise molecular architectures. Poly-L-lysine dendrimers with a cubic octa(3-aminopropyl)silsesquioxane (OAS) core, $(L\text{-lysine})_8$-OAS, $(L\text{-lysine})_{16}$-$(L\text{-lysine})_8$-OAS, $(L\text{-lysine})_{32}$-$(L\text{-lysine})_{16}$-$(L\text{-lysine})_8$-OAS, and $(L\text{-lysine})_{64}$-$(L\text{-lysine})_{32}$-$(L\text{-lysine})_{16}$-$(L\text{-lysine})_8$-OAS, were divergently synthesized by solution phase peptide chemistry in good yield and purity. Matrix-assisted laser desorption time of flight (MALDI-TOF) mass spectrometry showed complete substitution of the surface amino groups of lower generation dendrimers during synthesis, as well as precisely defined molecular architectures of the nanoglobules. The structures of the nanoglobules were further characterized by ^{1}H- and ^{13}C-NMR and 2D-NMR (correlation spectroscopy (COSY) and pulsed-field-gradient heteronuclear multiple quantum correlation (gHMQC)) spectroscopy. The ^{1}H-NMR spectroscopy revealed that the nanoglobules had a relatively rigid molecular architecture. Cytotoxicity studies showed that these nanoglobules exhibited a size-dependent toxicity, but it was much lower than that of linear poly-L-lysine. Preliminary in vitro nucleic acid delivery studies have shown that these globular dendrimers can efficiently deliver plasmid DNA to MDA-MB-231 cells. These nanoglobules hold much promise as safe drug carriers with precisely defined molecular architecture.

Keywords: Nanoglobules; lysine dendrimers; silsesquioxane; gene delivery; nanomaterials

Introduction

Rational design of synthetic macromolecules with precisely defined molecular architectures is of great interest in chemistry, biology, medicine, and nanotechnology. Dendrimers are highly branched macromolecules with well-controlled molecular architectures and highly functionalized outer layers.[1–4] The precise chemical composition and structure, and high chemical versatility, of dendrimers make them attractive in broad biomedical applications.[5,6] Biocompatible dendrimers have been used as carriers for the delivery of anticancer drugs,[7–9] DNA,[10,11] siRNA,[12] and imaging

* Correspondence to: Dr. Zheng-Rong Lu, 421 Wakara Way, Suite 318, Salt Lake City, UT 84108. Phone: 801 587-9450. Fax: 801 585-3614. E-mail: zhengrong.lu@utah.edu.

(1) Newkome, G. R.; Moorefield, C. N.; Vogtle, F. *Dendritic Molecules. Concepts, Syntheses, Perspectives*; VCH: Cambridge, England, 1996.

(2) Frechet, J. M. J., Tomalia, D. A., Eds. *Dendrimers and Other Dendritic Polymers*; Wiley: New York, 2001.

(3) Grayson, S. M.; Frechet, J. M. J. Convergent dendrons and dendrimers: from synthesis to applications. *Chem. Rev.* **2001**, *101*, 3819–3868, http://dx.doi.org/10.1021/cr990116h.

(4) Crespo, L.; Sanclimens, G.; Pons, M.; Giralt, E.; Royo, M.; Albericio, F. Peptide and Amide Bond–Containing Dendrimers. *Chem. Rev.* **2005**, *105*, 1663–1681, http://dx.doi.org/10.1021/cr030449I.

(5) Lee, C. C.; MacKay, J. A.; Frechet, J. M.; Szoka, F. C. Designing dendrimers for biological applications. *Nat. Biotechnol.* **2005**, *23*, 1517–1526, http://dx.doi.org/10.1038/nbt1171.

(6) Svenson, S.; Tomalia, D. A. Dendrimers in biomedical applications–reflections on the field. *Adv. Drug Deliv. Rev.* **2005**, *57*, 2106–2129, http://dx.doi.org/10.1016/j.addr.2005.09.018.

(7) Duncan, R.; Izzo, L. Dendrimer biocompatibility and toxicity. *Adv. Drug Deliv. Rev.* **2005**, *57*, 2215–2237, http://dx.doi.org/10.1016/j.addr.2005.09.019.

10.1021/mp070036z CCC: $37.00
Published on Web 08/17/2007

agents[13,14] in cancer treatment, gene therapy, and biomedical imaging. The conjugation of therapeutic agents and imaging agents onto the dendrimer surface results in size dependent modification of their pharmacokinetics,[15] which may improve the pharmacological outcome of these agents. Conventional dendrimers for biomedical applications are commonly prepared from bifunctional cores, e.g., ethylene diamine. Although these dendrimers possess a certain degree of spherical morphology, their structures are still relatively flexible.[16,17]

The majority of functional proteins have compact and globular molecular architectures. They function as enzymes (bioreactors or catalysts of biological reactions), transporters, DNA packing materials, etc. Biocompatible synthetic nanomolecules with symmetric and precisely defined globular molecular architectures have the potential to mimic biological functions of globular proteins and to specifically deliver bioactive agents for disease diagnosis and treatment. Currently, there are no such synthetic macromolecules available for biomedical research and applications. The design and synthesis of globular macromolecules with a precisely defined molecular architecture will result in novel nanomaterials for broad biomedical applications. In addition, one can expect that dendrimers with rigid and symmetric, globular architectures may have interesting physicochemical and biological properties.

Octasilsesquioxanes with the formula $R_8Si_8O_{12}$ have a unique three-dimensional cubic symmetry.[18–21] The cubic silsesquioxanes have a size of approximately 1 nm in diameter with eight functional R groups at each corner. Functionalized octasilsesquioxanes can be used as cores to prepare dendrimers with a true symmetric architecture. Dendrimer branches can divergently grow at the functional corners of the core in three-dimensions. Recently, a few dendrimers of low generations (up to 2) have been prepared from an octasilsesquioxane core.[22–25] These dendrimers exhibit a globular morphology and have high surface functionality.[26]

Biocompatible dendrimers prepared from a cubic octasilsesquioxane core may have some unique features for biomedical applications as compared to dendrimers with bifunctional, nonrigid cores. These dendrimers will have a

(8) Kukowska-Latallo, J. F.; Candido, K. A.; Cao, Z.; Nigavekar, S. S.; Majoros, I. J.; Thomas, T. P.; Balogh, L. P.; Khan, M. K.; Baker, J. R., Jr. Nanoparticle targeting of anticancer drug improves therapeutic response in animal model of human epithelial cancer. *Cancer Res.* **2005**, *65*, 5317–5324.

(9) Gillies, E. R.; Frechet, J. M. Dendrimers and dendritic polymers in drug delivery. *Drug Discov. Today* **2005**, *10*, 35–43, http://dx.doi.org/10.1016/S1359-6446(04)03276-3.

(10) Tang, M. X.; Redemann, C. T.; Szoka, F. C., Jr. In vitro gene delivery by degraded polyamidoamine dendrimers. *Bioconjugate Chem.* **1996**, *7*, 703–714, http://dx.doi.org/10.1021/bc9600630.

(11) Zhang, X. Q.; Wang, X. L.; Huang, S. W.; Zhuo, R. X.; Liu, Z. L.; Mao, H. Q.; Leong, K. W. In vitro gene delivery using polyamidoamine dendrimers with a trimesyl core. *Biomacromolecules* **2005**, *6*, 341–350, http://dx.doi.org/10.1021/bm040060n.

(12) Kang, H.; DeLong, R.; Fisher, M. H.; Juliano, R. L. Tat-conjugated PAMAM dendrimers as delivery agents for antisense and siRNA oligonucleotides. *Pharm Res.* **2005**, *22*, 2099–2106, http://dx.doi.org/10.1007/s11095-005-8330-5.

(13) Wiener, E. C.; Brechbiel, M. W.; Brothers, H.; Magin, R. L.; Gansow, O. A.; Tomalia, D. A.; Lauterbur, P. C. Dendrimer-based metal chelates: a new class of magnetic resonance imaging contrast agents. *Magn. Reson. Med.* **1994**, *31*, 1–8, http://dx.doi.org/10.1002/mrm.1910310102.

(14) Talanov, V. S.; Regino, C. A.; Kobayashi, H.; Bernardo, M.; Choyke, P. L.; Brechbiel, M. W. Dendrimer-based nanoprobe for dual modality magnetic resonance and fluorescence imaging. *Nano Lett.* **2006**, *6*, 1459–1463, http://dx.doi.org/10.1021/nl060765q.

(15) Kobayashi, H.; Kawamoto, S.; Jo, S. K.; Bryant, H. L., Jr; Brechbiel, M. W.; Star, R. A. Macromolecular MRI contrast agents with small dendrimers: pharmacokinetic differences between sizes and cores. *Bioconjugate Chem.* **2003**, *14*, 388–394, http://dx.doi.org/10.1021/bc025633c.

(16) Gorman, C. B.; Smith, J. C. Effect of repeat unit flexibility on dendrimer conformation as studied by atomistic molecular dynamics simulations. *Polymer* **2000**, 675–683, http://dx.doi.org/10.1016/S0032-3861(99)00167-6.

(17) Mazo, M. A.; Shamaev, M. Y.; Balabaev, N. K.; Darinskii, A. A.; Neelov, I. M. Conformational mobility of carbosilane dendrimer: Molecular dynamics simulation. *Phys. Chem. Chem. Phys.* **2004**, 1285–1289, http://dx.doi.org/10.1039/b311131h.

(18) Feher, F. J.; Soulivong, D.; Eklund, A. G. Controlled cleavage of R8Si8O12 frameworks: a revolutionary new method for manufacturing precursors to hybrid inorganic–organic materials. *Chem. Commun.* **1998**, 399–400, http://dx.doi.org/10.1039/a707061f.

(19) Kannan, R. Y.; Salacinski, H. J.; Butler, P. E.; Seifalian, A. M. Polyhedral oligomeric silsesquioxane nanocomposites: the next generation material for biomedical applications. *Acc. Chem. Res.* **2005**, *38*, 879, http://dx.doi.org/10.1021/ar050055b.

(20) Liang, K.; Toghiani, H.; Li, G.; Pittman, C. U., Jr. Synthesis, morphology, and viscoelastic properties of cyanate ester/polyhedral oligomeric silsesquioxane nanocomposites. *J. Polym. Sci., Part A: Polym. Chem.* **2005**, *43*, 3887, http://dx.doi.org/10.1002/pola.20861.

(21) Lee, A.; Xiao, J.; Feher, F. J. New Approach in the Synthesis of Hybrid Polymers Grafted with Polyhedral Oligomeric Silsesquioxane and Their Physical and Viscoelastic Properties. *Macromolecules* **2005**, *38*, 438–444, http://dx.doi.org/10.1021/ma047892y.

(22) Ropartz, L.; Foster, D. F.; Morris, R. E.; Slawin, A. M. Z.; Cole-Hamilton, D. J. Hydrocarbonylation reactions using alkylphosphine-containing dendrimers based on a polyhedral oligosilsesquioxane core. *J. Chem. Soc., Dalton Trans.* **2002**, 1997–2008, http://dx.doi.org/10.1039/b200303a.

(23) Hong, B.; Thoms, T. P. S.; Murfee, H. J.; Lebrun, M. J. Highly branched dendritic macromolecules with core polyhedral silsesquioxane functionalities. *Inorg. Chem.* **1997**, *36*, 6146–6147, http://dx.doi.org/10.1021/ic971034j.

(24) Feher, F. J.; Wyndham, K. K. Amine and ester-substituted silsesquioxanes: synthesis, characterization and use as a core for starburst dendrimers. *Chem. Commun.* **1998**, 323–324, http://dx.doi.org/10.1039/a707140j.

(25) Wada, K.; Watanabe, N.; Yamada, K.; Kondo, T.; Mitsudo, T. A. Synthesis of novel starburst and dendritic polyhedral oligosilsesquioxanes. *Chem. Commun.* **2005**, 95–97, http://dx.doi.org/10.1039/b413921f.

(26) Haxton, K. J.; Cole-Hamilton, D. J.; Morris, R. E. The structure of phosphine-functionalised silsesquioxane-based dendrimers: a molecular dynamics study. *J. Chem. Soc., Dalton Trans.* **2004**, 1665–1669, http://dx.doi.org/10.1039/b404260c.

denser, more symmetric molecular architecture. These features are ideal for targeted delivery of therapeutic genes, which can be incorporated into a dendrimer surface that better mimics biological proteins, such as histones. Here, we report the synthesis and characterization of symmetric L-lysine dendrimers with an octa(3-aminopropyl)silsesquioxane core (OAS) up to generation 4. Since these molecules have well-defined sizes at the nanoscale and globular molecular architectures, we have coined the term "nanoglobules" for these new molecules. Cytotoxicity and in vitro gene delivery of the nanoglobules was preliminarily evaluated with linear poly-L-lysine as a control.

Experimental Section

Materials. Octa(3-aminopropyl)silsesquioxane hydrochloride (OctaAmmonium POSS-HCl) was purchased from Hybrid Plastics (Hattiesburg, MS). 2-(1*H*-Benzotriazole-1yl)-1,1,3,3-tetramethyluronium hexafluorophosphate (HBTU), 1-hydroxy benzotriazole hydrate (HOBt), and N_α,N_ε-di-*t*-BOC-L-lysine dicyclohexylammonium salt [(di-t-BOC)$_2$-*L*-lys-OH·DCHA] were purchased from Nova Biochem (Darmstadt, Germany). *N*,*N*-diisopropylethylamine (DIPEA) and *N*,*N*-dimethylformamide anhydrous (DMF) were purchased from Alfa Aesar (Ward Hill, MA). Citric acid was purchased from J.T. Baker (Phillipsburg, NJ). Trifluoroacetic acid (TFA) was purchased from ACROS Organics (Morris Plains, NJ). All reagents and solvents for dendrimer preparation were used without further purification unless otherwise stated.

Methods. ^{1}H-NMR and ^{13}C-NMR spectra were acquired on a Varian INOVA 400 NMR spectrometer. Matrix-assisted laser desorption time of flight (MALDI-TOF) mass spectra were acquired on a Voyager DE-STR spectrometer (PerSpeptive BioSystems) in linear mode with α-cyano-4-hydroxycinnamic acid as a matrix. Sample purification was performed using high pressure liquid chromatography (HPLC) on an Agilent 1100 HPLC system equipped with a ZORBAX 300SB–C18 PrepHT column. The gradient mobile phase was a mixture of H_2O (0.05% TFA) and acetonitrile (0.05% TFA).

Preparation of (L-Lysine)$_8$-OAS (G$_1$). Octa(3-aminopropyl)silsesquioxane hydrochloride (0.70 g, 0.597 mmol), HBTU (7.60 g, 20.0 mmol), HOBt (2.70 g, 20.0 mmol), and (*t*-BOC)$_2$-*L*-lys-OH·DCHA (10.4 g, 20.0 mmol) were dissolved in 30 mL DMF. The reaction mixture was stirred at room temperature for 20 min in N_2 atmosphere. Diisopropylethylamine amine (10 mL) was added to the solution, and the mixture was stirred at room temperature for 2 days. The reaction mixture was added to a 0.5 M citric acid aqueous solution in an ice-bath giving a white, sticky precipitate. The precipitate was then treated with acetonitrile giving a colorless solid. The solid product was collected by filtration and dried under vacuum. Yield of [(*t*-BOC)$_2$-L-lysine]$_8$-OAS was 1.29 g, 61.6%. [(*t*-BOC)$_2$-L-lysine]$_8$-OAS (1.29 g) was dissolved in 5 mL ice-cold trifluoroacetic acid (TFA) and stirred at room temperature for 1 h to remove *t*-BOC groups. The solution was then concentrated under vacuum to a viscous oil. The residue was treated with ice-cold anhydrous diethyl ether giving a colorless solid product. The yield of (L-lysine)$_8$-OAS trifluoroacetate was 1.04 g (47.1%). The product was further purified by HPLC using a ZORBAX 300SB-C18 PrepHT column with a gradient of deionized water and acetonitrile containing 0.05% TFA. ^{1}H-NMR (D_2O, δ): 3.83 (t, 8H, –C*H*), 3.40–2.98 (dm, 16H, –Si(CH$_2$)$_2$C*H*$_2$), 2.84 (t, 16H, –(CH$_2$)$_3$C*H*$_2$), 1.74 (m, 16H, –CHC*H*$_2$), 1.58 (m, 16H, –(CH$_2$)$_2$C*H*$_2$CH$_2$), 1.47 (m, 16H, –SiCH$_2$C*H*$_2$), 1.31 (m, 16H, –CH$_2$C*H*$_2$(CH$_2$)$_2$), 0.54 (t, 16H, –SiC*H*$_2$). ^{13}C-NMR (D_2O, δ): 169.4 (8C, *C*O), 53.2 (8C, -*C*H), 42.0 (8C, –Si(CH$_2$)$_2$*C*H$_2$), 39.1 (8C, –(CH$_2$)$_3$*C*H$_2$), 30.6 (8C, –CH*C*H$_2$), 26.5 (8C, –(CH$_2$)$_2$*C*H$_2$CH$_2$), 21.8 (8C, –SiCH$_2$*C*H$_2$), 21.5 (8C, –CH$_2$*C*H$_2$(CH$_2$)$_2$), 8.39 (8C, –Si*C*H$_2$). MALDI-TOF (*m/z*, $[M + H]^+$): 1907.88 (calculated for $C_{72}H_{160}N_{24}O_{20}Si_8$), 1907.04 (measured).

Preparation of (L-Lysine)$_{16}$-(L-Lysine)$_8$-OAS (G$_2$). (L-Lysine)$_8$-OAS (G$_1$) trifluoroacetate (0.497 g, 0.133 mmol), HBTU (6.76 g, 17.8 mmol), HOBt (2.40 g, 17.8 mmol), and (*t*-BOC)$_2$-*L*-lys-OH·DCHA (9.40 g, 17.8 mmol) were dissolved in 20.0 mL DMF. The reaction was carried out similarly as described in the synthesis of (L-lysine)$_8$-OAS. The precipitate was then dissolved in methanol and purified by size exclusion chromatography using a column packed with Pharmacia LH-20 medium, eluted with methanol. The product fraction was collected, and a colorless solid, [(*t*-BOC)$_2$-L-lysine]$_{16}$-(L-lysine)$_8$-OAS (0.79 g, 83%), was obtained after the solvent was removed under vacuum. The product (0.79 g) was dissolved in 3 mL of ice-cold TFA to remove the *t*-BOC groups. Colorless (L-lysine)$_{16}$-(L-lysine)$_8$-OAS (G$_2$) trifluoroacetate was obtained in high yield (0.82 g, 80%). ^{1}H-NMR (D_2O, δ): 4.15 (t, 8H, –C*H*), 3.91 and 3.80 (dt, 16H, –C*H*), 3.20–2.91 (br 16H, –(CH$_2$)$_3$C*H*$_2$ and 16H, –Si(CH$_2$)$_2$C*H*$_2$), 2.84 (br m, 32H, –(CH$_2$)$_3$C*H*$_2$NH$_2$), 1.86–1.68 (br m, 32H, –CHC*H*$_2$ and 16H, –CHC*H*$_2$), 1.66–1.48 (br m, 32H, –(CH$_2$)$_2$C*H*$_2$CH$_2$ and 16H, –(CH$_2$)$_2$C*H*$_2$CH$_2$), 1.48–1.18 (br m, 32H, –CH$_2$C*H*$_2$(CH$_2$)$_2$, 16H, –CH$_2$C*H*$_2$(CH$_2$)$_2$, and 16H, –SiCH$_2$C*H*$_2$), 0.51 (br t, 16H, –SiC*H*$_2$). ^{13}C-NMR (D_2O, δ): 173.2 (8C, *C*O), 169.6–169.4 (16C, *C*O), 54.3 (8C, –*C*H), 53.2–52.9 (16C, –*C*H), 42.0 (8C, –Si(CH$_2$)$_2$*C*H$_2$), 39.5 (8C, –(CH$_2$)$_3$*C*H$_2$), 39.1 (16C, –(CH$_2$)$_3$*C*H$_2$), 31.1 (8C, –CH*C*H$_2$), 30.5 (16C, –CH*C*H$_2$), 28.1 (8C, –(CH$_2$)$_2$*C*H$_2$CH$_2$), 26.5–26.4 (16C, –(CH$_2$)$_2$*C*H$_2$CH$_2$), 22.8 (8C, –CH$_2$*C*H$_2$(CH$_2$)$_2$), 21.9 (8C, –SiCH$_2$*C*H$_2$), 21.5–21.4 (16C, –CH$_2$*C*H$_2$(CH$_2$)$_2$), 8.39 (8C, –Si*C*H$_2$). MALDI-TOF (*m/z*, $[M + H]^+$): 3958.64 (calculated for $C_{168}H_{352}N_{56}O_{36}Si_8$); 3958.49 (observed).

Preparation of (L-Lysine)$_{32}$-(L-Lysine)$_{16}$-(L-Lysine)$_8$-OAS (G$_3$). (L-Lysine)$_{16}$-(L-lysine)$_8$-OAS (G$_2$) trifluoroacetate (0.363 g, 0.0476 mmol), HBTU (4.45 g, 11.7 mmol), HOBt (1.58 g, 11.7 mmol), and (*t*-BOC)$_2$-*L*-Lys-OH·DCHA (6.17 g, 11.7 mmol) were dissolved in 12.0 mL DMF. The reaction procedure was similar to that of (L-lysine)$_{16}$-(L-lysine)$_8$-OAS. [(*t*-BOC)$_2$-L-lysine]$_{32}$-(L-lysine)$_{16}$-(L-lysine)$_8$-OAS was similarly isolated and purified as G$_2$. Yield: 0.483 g. 70%. The final product, (L-lysine)$_{32}$-(L-lysine)$_{16}$-(L-lysine)$_8$-OAS (G$_3$) trifluoroacetate, was obtained as a colorless solid in high yield (0.450 g, 61%) after deprotection in TFA. ^{1}H-NMR (D_2O,

δ): 4.25–4.08 (br, 16H, –C*H* and 8H, –C*H*), 3.91 and 3.80 (br m, 32H, –C*H*), 3.20–2.79 (br, 32H, $-(CH_2)_3CH_2$, 16H, $-(CH_2)_3CH_2$, 16H, $-Si(CH_2)_2CH_2$, and 64H, $-(CH_2)_3CH_2NH_2$), 1.95–1.10 (br, 64H, –CHC*H*$_2$, 32H, –CHC*H*$_2$, 16H, –CHC*H*$_2$, 64H, $-(CH_2)_2CH_2CH_2$, 32H, $-(CH_2)_2CH_2CH_2$, 16H, $-(CH_2)_2CH_2CH_2$, 16H, $-SiCH_2CH_2$, 64H, $-CH_2CH_2(CH_2)_2$, 32H, $-CH_2CH_2(CH_2)_2$ and 16H, $-CH_2CH_2(CH_2)_2$), 0.43 (t, 16H, –SiC*H*$_2$); ^{13}C-NMR (D_2O, δ): 174.0–173.3 (16C, *C*O and 8C, *C*O), 169.7–169.4 (32C, *C*O), 54.5–53.9 (16C, –*C*H and 8C, –*C*H), 53.3–52.8 (32C, –*C*H), 42.0 (8C, $-Si(CH_2)_2CH_2$), 39.5 (16C, $-(CH_2)_3CH_2$ and 8C, $-(CH_2)_3CH_2$), 39.1 (32C, $-(CH_2)_3CH_2$), 31.0–30.1 (32C, –CH*C*H$_2$, 16C, –CH*C*H$_2$, and 8C, –CH*C*H$_2$), 28.1–27.9 (16C, $-(CH_2)_2CH_2CH_2$, and 8C, $-(CH_2)_2CH_2CH_2$), 26.5 (32C, $-(CH_2)_2CH_2CH_2$), 23.1–22.2 (16C, $-CH_2CH_2(CH_2)_2$, 8C, $-CH_2CH_2(CH_2)_2$, and 8C, $-SiCH_2CH_2$), 21.5–21.3 (32C, $-CH_2CH_2(CH_2)_2$), 8.39 (8C, –Si*C*H$_2$). MALDI-TOF (*m/z*, $[M + H]^+$): 8059.97 (calculated for $C_{360}H_{736}N_{120}O_{68}Si_8$); 8059.05 (observed).

Preparation of (L-Lysine)$_{64}$-(L-Lysine)$_{32}$-(L-Lysine)$_{16}$-(L-Lysine)$_8$-OAS (G_4). (L-Lysine)$_{32}$-(L-lysine)$_{16}$-(L-lysine)$_8$-OAS (G_3) trifluoroacetace (0.176 g, 0.0114 mmol), HBTU (2.12 g, 5.50 mmol), HOBt (0.708 g, 5.60 mmol), and (*t*-BOC)$_2$-*L*-lys-OH·DCHA (2.95 g, 5.60 mmol) were dissolved in 10.0 mL DMF. The reaction procedure was similar to that of (L-lysine)$_{16}$-(L-lysine)$_8$-OAS. [(*t*-BOC)$_2$-L-lysine]$_{64}$-(L-lysine)$_{32}$-(L-lysine)$_{16}$-(L-lysine)$_8$-OAS was obtained as colorless solid after purification with SEC (0.25 g, 75%). (L-Lysine)$_{64}$-(L-lysine)$_{32}$-(L-lysine)$_{16}$-(L-lysine)$_8$-OAS (G_4) trifluoroacetate was also obtained as colorless solid in high yield (0.25 g, 70%) after deprotection by TFA. ^{1}H-NMR (D_2O, δ): 4.21–4.02 (br, 32H, –C*H*, 16H, –C*H*, and 8H, –C*H*), 3.91 and 3.78 (br 64H, –C*H*), 3.15–2.76 (br, 64H, $-(CH_2)_3CH_2$, 32H, $-(CH_2)_3CH_2$, 16H, $-(CH_2)_3CH_2$, 16H, $-Si(CH_2)_2CH_2$, and 128H, $-(CH_2)_3CH_2NH_2$), 1.83–1.06 (br, 128H, –CHC*H*$_2$, 64H, –CHC*H*$_2$, 32H, –CHC*H*$_2$, 16H, –CHC*H*$_2$, 128H, $-(CH_2)_2CH_2CH_2$, 64H, $-(CH_2)_2CH_2CH_2$, 32H, $-(CH_2)_2CH_2CH_2$, 16H, $-(CH_2)_2CH_2CH_2$, 16H, $-SiCH_2CH_2$, 128H, $-CH_2CH_2(CH_2)_2$, 64H, $-CH_2CH_2(CH_2)_2$, 32H, $-CH_2CH_2(CH_2)_2$, and 16H, $-CH_2CH_2(CH_2)_2$), 0.43 (br, 16H, –SiC*H*$_2$). ^{13}C-NMR (D_2O, δ): 174.0–173.3 (32C, *C*O, 16C, *C*O, and 8C, *C*O), 170.0–169.4 (64C, *C*O), 54.5–52.9 (64C, –*C*H, 32C, –*C*H, 16C, –*C*H, and 8C, –*C*H), 40.1–38.5 (64C, $-(CH_2)_3CH_2$, 32C, $-(CH_2)_3CH_2$, 16C, $-(CH_2)_3CH_2$, and 8C, $-(CH_2)_3CH_2$), 31.0–29.6 (64C, –CH*C*H$_2$, 32C, –CH*C*H$_2$, 16C, –CH*C*H$_2$, and 8C, –CH*C*H$_2$), 29.3 (16C, $-(CH_2)_2CH_2CH_2$), 28.0 (64C, $-(CH_2)_2CH_2CH_2$ and 32C, $-(CH_2)_2CH_2CH_2$), 23.6–22.2 (32C, $-CH_2CH_2(CH_2)_2$, 16C, $-CH_2CH_2(CH_2)_2$, 8C, $-CH_2CH_2(CH_2)_2$, and 8C, $-SiCH_2CH_2$), 21.5 (64C, $-CH_2CH_2(CH_2)_2$. MALDI-TOF (*m/z*, $[M + H]^+$): 16263.18 (calculated for $C_{744}H_{1504}N_{248}O_{152}Si_8$); 16314.96 (observed).

Cytotoxicity Assay. The cytotoxicity of each dendrimer generation was evaluated using a modified 3-(4,5-dimethylthiazol-2-yl)-2,5-diphenyltetrazolium bromide (MTT) assay.[27,28] MDA-MB-231 cells were seeded into 96-well microtiter plates 24 h before the assay at a density of 10 000 cells/well. The cells were incubated at 37 °C with Leibovitz L-15 medium containing dendrimer generations at different concentrations: 1.5, 3.12, 6.25, 12.5, 25, 50, 100, and 200 μg/mL for 48 h. Poly-L-lysine (10 kDa) and the OAS core were used as controls. The medium in each well was replaced with 100 μL of fresh medium. A 25 μL portion of MTT solution in PBS was added, and the cells were incubated for another 4 h. The media was removed, 200 μL of DMSO was added to each well, and the cells were incubated at 37 °C for an additional 5 min. The optical densities were measured at 570 nm using a microplate reader (Model 550, Bio-Rad Laboratory, Hercules, CA). The relative cell viability was calculated by the following equation: $([Abs]_{sample} - [Abs]_{blank})/([Abs]_{control} - [Abs]_{blank}) \times 100\%$.

Gel Electrophoresis Shift Assay. The ability of generations 1–4 nanoglobules, as well as the OAS core, to complex DNA was examined by gel electrophoresis. Agarose gel (0.8%, w/v) containing 0.5 μg/mL ethidium bromide was prepared in TAE (tris-acetate-EDTA) buffer. DNA (10 μL, 0.1 μg/μL) was mixed with an equal volume of polymer solution at predetermined *N*/*P* ratios (*N* = polymer nitrogens that can be protonated, *P* = phosphate groups on DNA) and incubated for 30 min before use. Each sample (10 μL) was mixed with 2 μL of 6× loading dye, and the mixture was loaded onto an agarose gel. The gel was run at 100 V for 45 min. The location of DNA bands was visualized on a UV illuminator.

In Vitro Transfection Protocol. In vitro DNA delivery was investigated in MDA-MB-231 (human breast adenocarcinoma epithelial cells; American type Culture Collection, Rockville, MD) using the firefly luciferase plasmid as the reporter gene. MDA-MB-231 cells were maintained in ATCC Leibovitz's L-15 medium supplemented with 10% fetal bovine serum (FBS, HyClone, Logan, UT), streptomycin (100 μg/mL), and penicillin (100 units/mL). Cells were seeded 24 h prior to transfection into a 24-well plate. At the time of transfection, the medium in each well was replaced with 1 mL of serum-free medium. The nanoglobule/luciferase plasmid or SuperFect/luciferase plasmid at different *N*/*P* ratios were allowed to form polyplexes at room temperature for 30 min and then incubated with the cells for 4 h at 37 °C. The medium was then replaced with 1 mL of fresh complete medium and cells were incubated for an additional 48 h. Each *N*/*P* ratio was evaluated in triplicate. After incubation, cells were treated with 200 μL of cell lysis buffer (Promega Co., Madison, WI), followed by freeze-fracture. Luciferase gene expression was measured using a luciferase

(27) Lu, Z.-R.; Kopeckova, P.; Kopecek, J. Polymerizable Fab' antibody fragments for targeting of anticancer drugs. *Nature Biotechnol.* **1999**, *17*, 1101–1104, http://dx.doi.org/10.1038/15085.

(28) Choi, J. S.; Lee, E. J.; Choi, Y. H.; Jeong, Y. J.; Park, J. S. Poly(ethylene glycol)-block-poly(L-lysine) dendrimer: novel linear polymer/dendrimer block copolymer forming a spherical water-soluble polyionic complex with DNA. *Bioconjugate Chem.* **1999**, *10*, 62–65, http://dx.doi.org/10.1021/bc9800668.

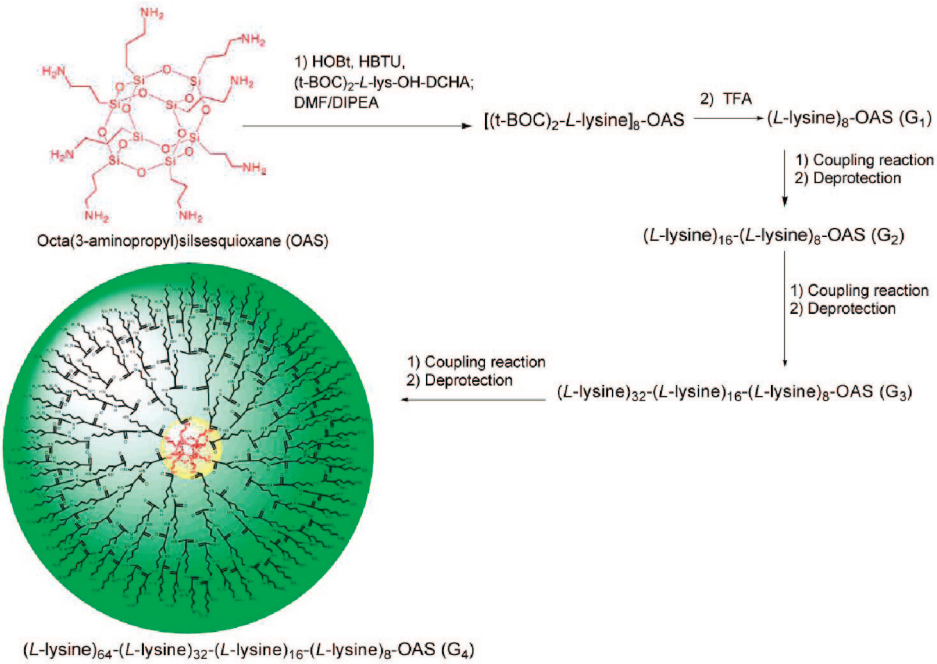

Figure 1. Synthetic scheme for the preparation of nanoglobules.

assay kit (Promega Co., Madison, WI) on a luminometer for 10 s (Lumat 9605, EG&G Wallac). The relative light units (RLU) were normalized against protein concentration in the cell extracts, measured by a BCA protein assay kit (Pierce, Rockford, IL). Luciferase activity was expressed as relative light units (RLU/mg of protein in the cell lysate).

Results and Discussion

Synthesis of Nanoglobules. Nanoglobules, three-dimensional dendrimers, were synthesized using liquid phase peptide synthesis[29] with octa(3-aminopropyl)silsesquioxane as the initial core. The synthetic scheme is shown in Figure 1. A large excess of N_α,N_ε-di-*t*-BOC-L-lysine-OH·DCHA and coupling agents were used in each step to ensure complete reaction of the surface amino groups with protected L-lysine. Diisopropylethylamine (DIPEA) was used to obtain free amino groups on the dendrimer surface by neutralizing the hydrochloride salt of the OAS core, or the trifluoroacetate salts of lower dendrimer generations. The branches of the starburst dendrimers expanded divergently in three dimensions from the eight corners of the cubic OAS core. [(*t*-BOC)$_2$-L-lysine]$_8$-OAS was isolated from the reaction mixture by precipitating in citric acid aqueous solution since the *t*-Boc protected nanoglobules exhibited low water solubility. The G_1 nanoglobule also exhibited low solubility in acetonitrile and a high purity product was obtained by washing the crude precipitate with acetonitrile as shown in the HPLC analysis. Since [(*t*-BOC)$_2$-L-lysine]$_{16}$-(L-lysine)$_8$-OAS, [(*t*-BOC)$_2$-L-lysine]$_{32}$-(L-lysine)$_{16}$-(L-lysine)$_8$-OAS, and [(*t*-BOC)$_2$-L-lysine]$_{64}$-(L-lysine)$_{32}$-(L-lysine)$_{16}$-(L-lysine)$_8$-OAS had a relatively larger size, they were readily purified by size exclusion chromatography after precipitation in aqueous solution. Generations 1–4 of the *t*-BOC protected dendrimers were obtained in good yield (60–80%) and high purity. L-Lysine-OAS dendrimers of generations 1–4 were also obtained in high yield and purity after the removal of *t*-BOC protecting groups with TFA. Synthesis of each generation was closely monitored by analytical HPLC, ^{1}H-NMR, and MALDI-TOF mass spectrometry.

Structural Characterization. The structure of the nanoglobules was characterized by ^{1}H-NMR, ^{13}C-NMR and 2D NMR (COSY and gHMQC), and matrix-assisted laser desorption ionization time of flight (MALDI-TOF). The NMR and mass spectra of the *t*-BOC-L-lysine dendrimers are complicated, possibly due to the partial deprotection during the precipitation in the citric acid solution. Clean NMR and mass spectra were obtained for the deprotected L-lysine nanoglobules and used for structural characterization.

The molecular ion peaks corresponding to the calculated mass were identified for G_1, G_2, and G_3 in the MALDI-TOF mass spectra of the L-lysine dendrimers. The molecular ion peak of the G_4 dendrimer had a mass (*m*/*z*) of 16 314.96, which was larger than the calculated mass (*m*/*z* ([M + H]$^+$ = 16 263.18). The slightly greater observed molecular weight might be attributed to the association of other molecules during MALDI-TOF MS analysis. Different molecular masses were observed for G_4 dendrimers during repeated acquisitions of the mass spectra, which might provide evidence for the formation of molecular associates. Nonetheless, mass spectrometric measurements revealed complete substitution of the surface amino groups of lower generation dendrimers in the coupling reaction. The results confirmed

(29) Zloh, M.; Ramaswamy, C.; Sakthivel, T.; Wilderspin, A.; Florence, A. T. Investigation of the association and flexibility of cationic lipidic peptide dendrons by NMR spectroscopy. *Magn. Reson. Chem.* **2005**, *43*, 47–52, http://dx.doi.org/10.1002/mrc.1508.

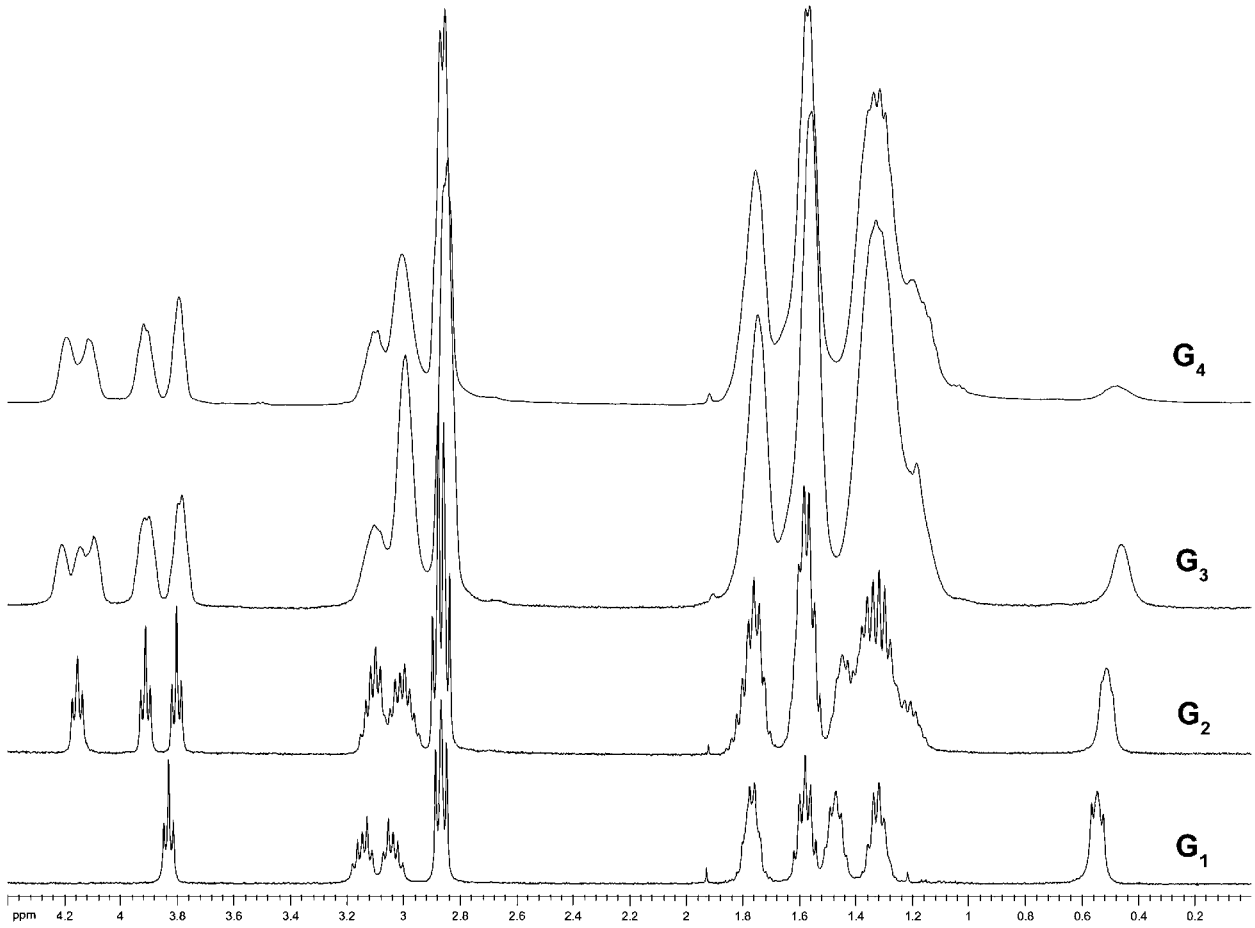

Figure 2. ^{1}H-NMR spectra at 400 MHz of the nanoglobules of G_1–G_4 in D_2O.

that unimolecular L-lysine-OAS dendrimers up to generation 4 were prepared by divergent synthetic chemistry.

^{1}H-NMR spectra of the dendrimers are shown in Figure 2. In the spectrum of G_1, the peak at 0.54 ppm is characteristic of the methylene proton adjacent to the silicon atoms of the OAS core. The position of this peak shifted slightly upfield on the ^{1}H-NMR spectrum and became broader as the generation number increased. The adjacent methylene protons appeared as multiplets at 1.47 ppm and later became masked by the increasing methylene protons of the L-lysine side chains of higher dendrimer generations. The β-protons, δ-protons, and γ-protons of the L-lysine side chain appeared as three multiplets at 1.77, 1.58, and 1.31 ppm, respectively, in the spectrum of the G_1 dendrimer. These peaks became broader at higher generations. The β-protons and δ-protons of the L-lysine side chain in the inner layer shifted upfield after subsequent conjugation of an exterior L-lysine layer. This was confirmed by 2D COSY NMR of G_2 and G_3 but was not evident on the G_4 spectrum due to the broadness of the lysine side chain peaks as well as the overwhelming signal from the exterior lysine residues. This phenomenon most likely results from chemical shielding of the interior L-lysine residues by the exterior L-lysine layer.[30] The γ-protons of the L-lysine side chain did not shift upfield after further addition of L-lysine to the dendrimer exterior. The ε-protons of the L-lysine were assigned to 2.84 ppm. This peak dramatically increases in height and becomes much broader in the ^{1}H-NMR spectra of generation 1–4 because the number of the exterior ε-protons increases from 16 to 128.

An interesting observation was the presence of two multiplets at 3.04 and 3.13 ppm for G_1. These two peaks were assigned to the two methylene protons ($H_{\gamma\text{-OAS}}$) adjacent to the nitrogen atom of the OAS core. The peak height ratio was 1 ($8H_{\gamma\text{-OAS}}$):1 ($8H_{\gamma\text{-OAS}}$). Upon addition of a second L-lysine generation, the two methylene protons adjacent to the nitrogen atom of the OAS core shifted slightly upfield to approximately 2.95 and 3.11 ppm, while the ε-protons ($H_{\varepsilon\text{-Lys1}}$) adjacent to the newly formed ε-amide bond of the first L-lysine generation were also present as two split peaks at 2.95 and 3.11 ppm. 2D COSY ^{1}H-NMR as well as pulsed-field-gradient heteronuclear multiple quantum correlation (gHMQC) NMR aided in clarifying the ^{1}H-NMR spectrum. In other words, the ε-protons of the first generation L-lysine side chain shifted downfield and were present as two split

(30) Baigude, H.; Katsuraya, K.; Okuyama, K.; Tokunaga, S.; Uryu, T. Synthesis of sphere-type monodispersed oligosaccharide-polypeptide dendrimers. *Macromolecules* **2003**, *36*, 7100–7106, http://dx.doi.org/10.1021/ma030021o.

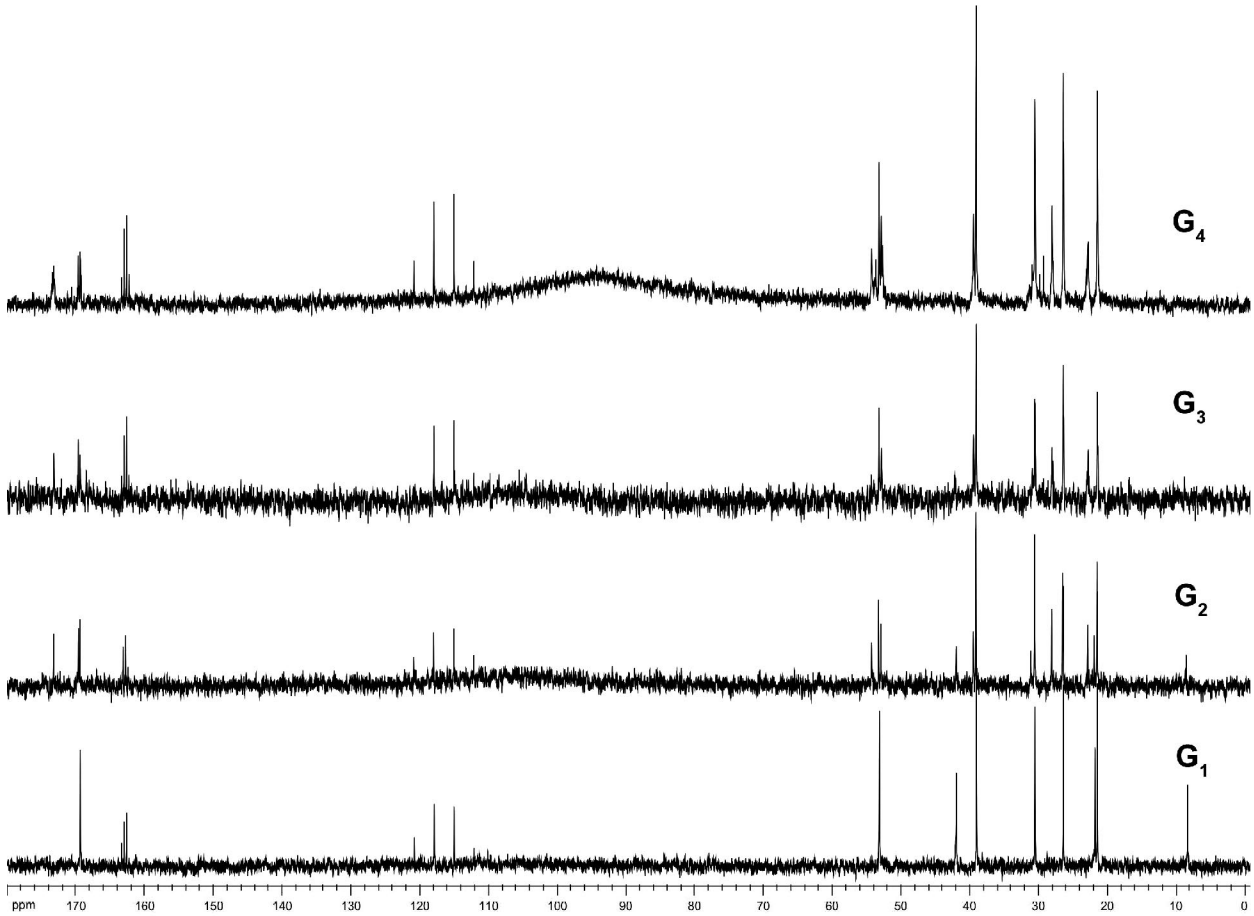

Figure 3. ^{13}C-NMR spectra at 400 MHz of the nanoglobules of G_1–G_4 in D_2O.

peaks after the second generation of L-lysine was conjugated to the dendrimer exterior. Although the methylene protons adjacent to the nitrogen atom of the OAS core shifted slightly upfield, these two peaks overlapped with the ε-protons of the first L-lysine generation. Consequently, a 1 ($8H_{\gamma\text{-OAS}}$ + $8H_{\varepsilon\text{-Lys1}}$):1 ($8H_{\gamma\text{-OAS}}$ + $8H_{\varepsilon\text{-Lys1}}$) peak height ratio in the ^{1}H-NMR spectrum of generation 2 was observed for the two peaks at 2.95 and 3.11 ppm. A similar trend was observed in the ^{1}H-NMR spectrum of generation 3 after a third L-lysine layer was conjugated to the surface. The ε-protons ($H_{\varepsilon\text{-Lys2}}$) adjacent to the newly formed amide bond were split into two peaks at approximately 2.95 and 3.11 ppm. The ε-protons of the first L-lysine residues and the methylene protons adjacent to the amide bond of the OAS core were all slightly shifted upfield to approximately 2.95 ppm. Consequently, the height ratio of the two peaks at 2.95 and 3.11 ppm was approximately 3 ($16H_{\varepsilon\text{-Lys2}}$ + $16H_{\varepsilon\text{-Lys1}}$ + $16H_{\gamma\text{-OAS}}$):1 ($16H_{\varepsilon\text{-Lys2}}$). A similar trend was observed in the ^{1}H-NMR spectrum of generation 4. However, it was difficult to precisely assign the chemical shift of the protons in both ^{1}H-NMR and 2D-NMR because the peaks became broader and more overlapped and the signal of the protons in the inner layers was very weak.

The presence of the two multiplet peaks of the inner layer methylene protons adjacent to the amide bond is indicative of a more rigid globular structure. The compact, three-dimensional molecular architecture and consequent steric effect most likely contributes to the rigidity of the dendrimers. Because of the compact space and steric hindrance, the chemical bonds around the methylene group, particularly the C–N bond, could not rotate freely, rendering the protons confined in different chemical environments. Consequently, two multiple peaks were observed for these protons. However, such a phenomenon was not observed in the ^{1}H-NMR spectra of L-lysine dendrimers synthesized from two-dimensional cores. For example, the methylene protons adjacent to the amide bond of L-lysine dendrimers synthesized from a single L-lysine residue[30] and ethylenediamine[31] core were represented by a triplet peak, because these dendrimers were much less rigid and the bonds around the methylene group could rotate freely. In comparison, the rigid structure of the nanoglobules limited such rotation and resulted in two multiplet peaks of the methylene protons.

The peak at 3.83 ppm in the ^{1}H-NMR spectrum of G_1 was assigned to the α-proton adjacent to the peptide bond. This peak moves downfield to ca. 4.15 ppm as a second generation of L-lysine is conjugated to the dendrimer surface.

(31) Feher, F. J.; Wyndham, K. D.; Soulivong, D.; Nguyen, F. Syntheses of highly functionalized cube-octameric polyhedral oligosilsesquioxanes ($R_8Si_8O_{12}$). *J. Chem. Soc., Dalton Trans.* **1999**, 1491, http://dx.doi.org/10.1039/a807302c.

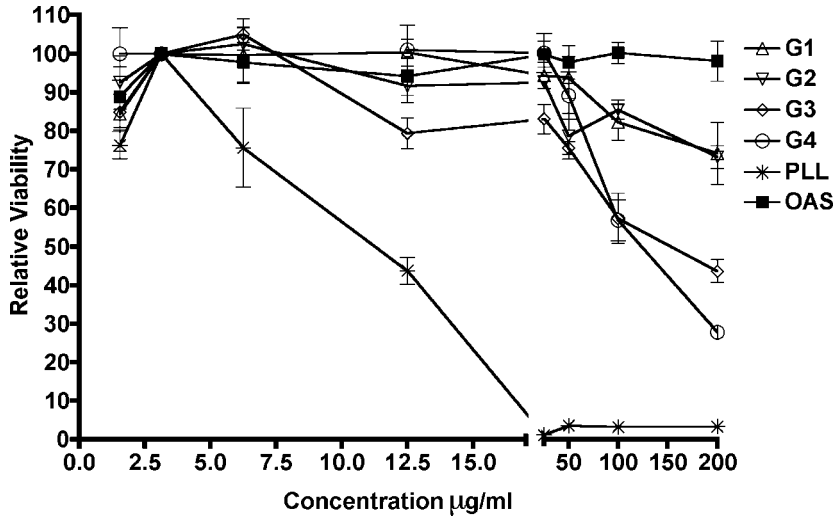

Figure 4. MTT cytotoxicity assay of the nanoglobules of G_1–G_4, as well as the OAS core and poly-L-lysine (10 kDa) in MDA-MB-231 cells: $N = 3$.

The α-protons of the surface L-lysine residues in G_2 dendrimer appeared as two distinct triplets at 3.80 and 3.91 ppm because of the different chemical environment after the conjugation to the α- and ε-animo groups of the L-lysine residue of G_1 dendrimers. Again, these two peaks shifted downfield to 4.09 and 4.14 ppm in the G_3 dendrimer, while the α-protons of the newly conjugated exterior L-lysine residues had split chemical shift values of 3.80 and 3.91 ppm. This trend was also observed after the conjugation of the fourth layer of L-lysine residues to the dendrimer exterior. The shift of α-protons of the inner layer L-lysine residue was also observed in the ^{1}H-NMR spectra of L-lysine dendrimers prepared with a two-dimensional core.[31]

Figure 3 shows the ^{13}C-NMR spectra of G_1–G_4. The peak at ca. 8.39 ppm is representative of the methylene carbon adjacent to the silicon atom, which retains the same chemical shift from G_1 to G_2. However, this peak is faintly shown in the G_3 spectrum and is not observed in the G_4 spectrum due to its low signal to noise ratio. The adjacent methylene carbon of the OAS core appeared at 21.9 ppm but was not observed in the spectra of G_3 and G_4. The methylene carbon of the OAS core that was adjacent to the amide bond was assigned to the peak at 42.0 ppm. This peak is present in the ^{13}C-NMR spectra of G_1–G_3; however, it is not seen in the spectrum of G_4 due to the low signal to noise ratio. The α-carbon of G_1 dendrimer appeared at 53.2 ppm and then shifted downfield to 54.2 ppm after the second L-lysine generation was conjugated to the surface. The α-carbons on the newly conjugated L-lysine of G_2 appeared as two peaks at 53.2 and 52.8 ppm. This trend was also observed for G_3 and G_4 dendrimers, which is similar to the α-protons in the ^{1}H-NMR spectra. The α-carbons of the surface L-lysine in G_3 appeared at ca. 53.3 and 52.8 ppm, while the α-carbons of interior lysine residues shifted downfield to 54.4 and 53.9 ppm, respectively. Again, the α-carbons of the L-lysine branches of G_3 shifted downfield to 54.0 ppm, while α-carbons of the surface L-lysine branches of G_4 appeared as two peaks at 53.2 and 52.9 ppm. The ε-, β-, δ-, and γ-carbons of the L-lysine side chains appeared at 39.1, 30.6, 26.4, and 21.5 ppm, respectively, in the spectrum of the G_1 dendrimer. Their chemical shift values moved slightly downfield after further conjugation of an outer L-lysine layer. The ε-, β-, δ-, and γ-carbons of the exterior L-lysine side chains were represented by similar chemical shift values as the previous interior L-lysine residues. In the ^{13}C-NMR spectrum of G_1, the peak at 169.0 ppm was assigned to the carbonyl carbon, which is the most deshielded carbon. The carbonyl carbon of the first generation of L-lysine moves downfield to ca. 173.0 ppm upon further conjugation of L-lysine, which is represented by a chemical shift at ca. 169.0 ppm. This trend is repeated through G_4.

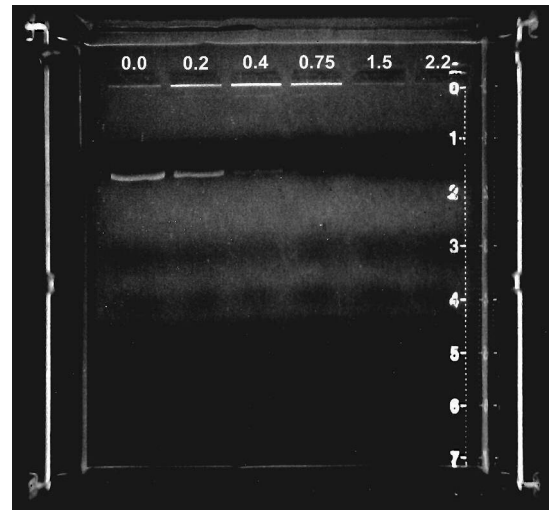

Figure 5. Gel retardation assay of generation 4 nanoglobule. Full DNA retardation is observed at an *N*/*P* ratio of 0.4–2.2. At high *N*/*P* ratios, generation 4 nanoglobules are capable of complexing and excluding the interchelating agent ethitium bromide.

Cytotoxicity. Toxicity is a crucial safety index for biomedical applications of these nanoglobules. Cytotoxicity

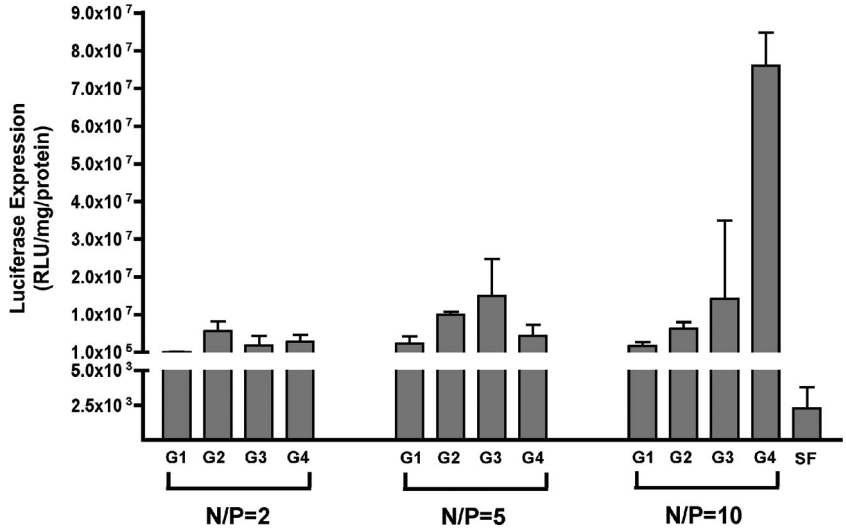

Figure 6. In vitro luciferase gene transfection in MDA-MB-231 cells. Nanoglobules generations 1–4 were incubated with serum-free media for 30 min at varying *N*/*P* ratios. The commercial transfection agent SuperFect (SF) was used as a control. The relative light intensity was normalized to total protein content by BCA assay: $N = 3$.

of the dendrimers and the octa(3-aminopropyl)silsesquioxane core was evaluated by incubation with MDA-MB-231 human breast carcinoma cells with poly-L-lysine (10 kDa) as a control. Figure 4 shows the concentration dependent cell viability of the OAS core, nanoglobular dendrimers, and poly-L-lysine. Each dendrimer generation and the core exhibited much lower cytotoxicity than poly-L-lysine. The cytotoxicity of the dendrimers gradually increases with their size. The IC_{50} values for G_3 and G_4 dendrimers were 134.8 μg/ml and 97.9 μg/ml, respectively, which is much higher than that of poly-L-lysine (12.0 μg/ml). IC_{50} values for the OAS core, G_1, and G_2 could not be calculated because the highest tested concentration (200 μg/mL) did not result in 50% inhibition of cell growth. The results indicate that these nanoglobules have low toxicity for biomedical applications.

Gel Retardation Assay. The ability of polycationic polymers to complex DNA into polyplexes is one perquisite for efficient DNA transfection. Nanoglobule DNA complexation efficiency was investigated with plasmid DNA encoding luciferase. Nanoglobules of generations 2–4 had a similar capacity to retard plasmid DNA. These molecules resulted in partial plasmid retardation at *N*/*P* ratios of approximately 0.5 and complete retardation at *N*/*P* ratios equal to, or higher than, 0.75 in gel electrophoresis assay. Figure 5 shows the DNA retardation of plasmid DNA with G_4 nanoglobules. G_1 dendrimers showed complete DNA retardation at an *N*/*P* ratio of 1.5, while the OAS core was incapable of retarding DNA at the *N*/*P* ratio of 1.5. In addition, at *N*/*P* ratios of 1.0 or higher, nanoglobules of generations 2–4 were capable of fully complexing DNA, which lead to the exclusion of ethidium bromide and a complete loss of fluorescence bands.

In Vitro Transfection. In vitro transfection efficiency of generation 1–4 nanoglobules was investigated in MDA-MB-231 breast carcinoma cells with a commercially available transfection agent, SuperFect, as a control. The OAS core was not evaluated due to inefficient DNA binding. The gWiz plasmid DNA expressing luciferase was used as a reporter gene. Figure 6 shows the transfection efficiency of G_1–G_4 at *N*/*P* ratios of 2, 5, and 10. No significant difference in transfection efficiency was observed at *N*/*P* ratios of 2 and 5 among the nanoglobules of different generations. However, G_4 had much greater transfection efficiency as compared to G_1, G_2, and G_3 nanoglobules at a *N*/*P* ratio of 10. All nanoglobule generations were more efficient at transfecting MDA-MB-231 cells than SuperFect.

Unlike linear polycations, where the polyplexes consist of an intertwining of polymer and DNA, we hypothesize that these nanoglobules bind and wrap DNA onto its surface. This mechanism of DNA compaction is analogous to histone proteins. The greater luciferase expression at the higher *N*/*P* ratio may be a result of better DNA compaction, which facilitates cellular entry and minimizes degradation. Although further studies are required, a plausible explanation for more efficient DNA compaction and protection is the similar physical properties between histone proteins and generation 4 nanoglobules. Further detailed nucleic acid delivery studies, including complexation of DNA with the nanoglobules, cellular uptake and polyplex size determination, and structural modification of the nanoglobules, are ongoing to better understand the structure–activity relationships of the dendrimers in gene delivery.

These novel nanoglobules may be advantageous for the application in biomedicine and nanotechnology as compared to other synthetic polymers, including dendrimers with flexible two-dimensional cores. For polymers with flexible structures, chemical modifications often result in a dramatic change in their morphology, i.e. hydrodynamic volume, which makes it difficult to prepare biomedical polymers with well-defined structures. Besides gene delivery, these nanoglobules can also be used as carriers for biomedical imaging and drug delivery. The highly functionalized surfaces can

be readily modified for various applications. Imaging agents, anticancer drugs, and targeting agents can be readily conjugated to the surface of the nanoglobules to prepare targeted imaging agents or drug delivery systems. Unlike flexible polymers, bioconjugation and modification at the surface will not significantly change the morphology of these nanoglobules.

Conclusion

Novel, three-dimensional L-lysine dendrimers with the cubic OAS core, nanoglobules, up to generation 4 were prepared by divergent synthesis in good yield and high purity with solution phase peptide chemistry. Their structures were characterized by ^{1}H-NMR and ^{13}C-NMR, as well as MALDI-TOF mass spectrometry. Mass spectrometric measurement confirmed complete substitution of the amino groups during the synthesis of higher dendrimer generation. ^{1}H-NMR studies indicated that the globular dendrimers had a relatively rigid chemical structure. The preliminary toxicity evaluation predicted the excellent biocompatibility of the nanoglobules. Gel retardation assays showed that these molecules effectively bound and retarded the migration of DNA at low *N*/*P* ratios. Furthermore, the nanoglobules were capable of effective in vitro gene delivery and transfection in MDA-MB-231 cells. These novel nanosized biomaterials with precisely defined molecular architectures hold great promise for applications in nanotechnology and nanomedicine.

Acknowledgment. This research was supported in part by the NIH R01 CA097465. We greatly appreciate Drs. Chad Nelson, Parsawar Krishna, and Mike Hanson of the University of Utah Core Facility Mass Spectrometry Lab, as well as Mr. Jay Olsen for his assistance and expertise in NMR.

MP070036Z